Nucleation and Growth of the Supercooled Liquid Phase Control Glass Transition in Bulk Ultrastable Glasses

A. Vila-Costa,[1] J. Ràfols-Ribé,[1,*] M. González-Silveira,[1] A. F. Lopeandia,[1] Ll. Abad-Muñoz,[2] and J. Rodríguez-Viejo[1,†]

[1]*Group of Nanomaterials and Microsystems, Physics Department, Universitat Autònoma de Barcelona, Bellaterra 08193, Spain*

[2]*Instituto de Microelectrónica de Barcelona—Centre Nacional de Microelectrònica, Campus UAB, Bellaterra, Barcelona 08193, Spain*

(Received 3 August 2019; accepted 7 January 2020; published 21 February 2020)

We report the anomalous bulk transformation of vapor deposited stable glasses into the liquid state. The transformation proceeds through two competing parallel processes: partial rejuvenation of the stable glass and nucleation and growth of liquid patches within the glass. The kinetics of the transformation extracted from heat capacity curves after isothermal runs is dominated by the heterogeneous nucleation and growth process that initiates at preexisting seeds and propagates radially at a velocity proportional to the alpha relaxation time. Remarkably, the distance between the activation seeds is independent of temperature within experimental uncertainty and amounts to several micrometers, a value in close agreement with the crossover length for TPD glasses. We speculate the initiation sites for the transformation of the glass into the supercooled liquid are localized regions of lower stability (or density).

DOI: 10.1103/PhysRevLett.124.076002

After more than a century of intense research the glass transition is still poorly understood and many different theories have been devised to understand its phenomenology. The glass transition measured at the laboratory has no identifiable structural signatures but is the result of an impressive reduction of the dynamics of the supercooled liquid by 12–14 orders of magnitude in a relatively small temperature window [1]. The kinetic nature of the glass transition and the existence of memory effects that result in hysteresis upon cooling and heating add complexity to the analysis. One of the first attempts to comprehend the influence of the thermal history on the properties of the glass was the phenomenological description by the Tool-Narayanaswami-Moynihan model [2] that introduced mean-field equations of motion for the fictive temperature (T_f) of the glass. Later on, other approaches such as kinetic constraint models [3] or random first-order theory (RFOT) [4] have been able to accurately reproduce calorimetric measurements with variable heating and cooling rates [5,6]. These theories are based on active regions of high mobility that catalyze the mobility of the nearby low-mobility (inactive) regions leading to propagating fronts. The difference in mobility is linked to a local field, spatially resolved, of the relaxation times (τ) or the local fictive temperatures in the glass. Previous experimental work has shown the transformation of highly stable thin film glasses into the supercooled liquid SCL proceeds through a moving front that propagates from surfaces to interfaces at a constant velocity that depends on the relaxation time of the liquid and on the stability of the glass [7,8]. If the film is thick enough or if the front is suppressed, the transformation occurs mainly in the interior of the glass [7,9]. The bulklike transformation of stable glasses has not been experimentally analyzed in detail yet. The only experimental work addressing it was in the original discovery of the front transformation where the kinetics of the bulk process was identified as Avrami type [7]. The transformation of stable glasses by moving fronts starting at surfaces, at inner regions of high mobility, or at nucleation sites has been discussed in detail in several theoretical and computational works [6,10–13]. Gutierrez and Garrahan [10] used a three dimensional East model with soft constraints to recreate the front and bulk transformation in stable glasses. Wolyness *et al.* [6,11] described the existence of moving fronts within RFOT by an analogy to a combustion process. On the other hand, Jack and Berthier used a triangular plaquette model to identify the transformation of stable glasses with a nucleation-and-growth process having large distances between nucleation events [12]. In a more recent work, the swap methodology [14] has enabled Berthier and co-workers to produce simulated glasses with stabilities that compare well to the highly stable glasses created in the laboratory by vapor deposition [15,16]. These simulated stable glasses transform into the liquid by moving fronts and if made thick enough a competing transformation between bulk and front or only a bulk process is observed [13].

Here, we report the kinetics of the bulklike transformation into the supercooled liquid of highly stable glasses of $N,N\_$-bis(3-methylphenyl)$-N,N\_$-bis(phenyl)-benzidine (TPD), glass transition temperature, $T_g = 333$ K, grown

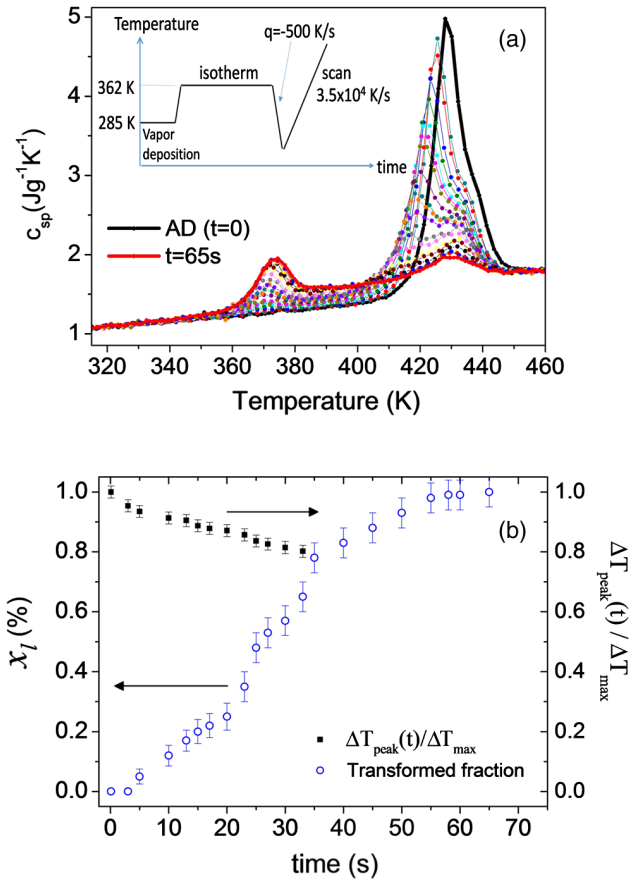

FIG. 1. (a) Specific heat as a function of temperature for as-deposited stable glasses grown at $T_{\mathrm{dep}} = 285\ K$ (continuous black line) and glasses undergoing partial transformations at $T_g + 29$ K. Annealing times range from 3-to-5 s between 0 and 65 s. The red curve represents a TPD glass totally transformed into supercooled liquid. (b) Calculated transformed fraction (left axis, blue open circles) and the ratio between the peak temperature shift of the stable TPD glass over time $\Delta T_{\mathrm{peak}}(t)$ and the maximum T_{peak} variation, $\Delta T_{\mathrm{max}} = T_{\mathrm{peak}}(t=0) - T_{\mathrm{peak}}(\mathrm{FC})$ (right axis, black solid squares) as a function of annealing time.

from the vapor at $0.85\,T_g$ during isothermal annealing at temperatures ranging from 347 to 367 K. The transformed fraction is described through the Kolmogorov-Johnson-Mehl-Avrami-Erofeev (KJMAE) formalism [17–20]. The exponents of the transformed fraction, $n \approx 2$ for thin films and $n \approx 3$ for bulk glasses, reveal the liquid forms at $t = 0$ at preexisting sites of the glass. Considering that the liquid propagates with a velocity that matches previous experimental data obtained for the front transformation, the distance between initiation sites amounts to $2.5 \pm 1\ \mu$m and is within experimental uncertainty independent of the annealing temperature.

We use fast scanning nanocalorimetry combined with isothermal treatments above T_g to investigate the amount of glass that transforms into SCL as a function of time. Since heat capacity measurements by nanocalorimetry involve the use of very thin films, the analysis of the bulk transformation requires the suppression of the front mechanism by eliminating highly mobile surfaces or interfaces. This is done by capping the thin film stable glass with a higher T_g material [21]. A full description of this procedure and its consequences on the heat capacity signature can be found elsewhere [9]. Briefly, after capping, the endothermic overshoot of the heat capacity related to the devitrification of the stable glass can be fully ascribed to a bulk transformation process. We choose tris(4-carbazoyl-9-ylphenyl) amine (TCTA, $T_g = 424$ K) as an effective capping layer for TPD [9]. Both materials TPD (85 nm thick) and TCTA (12 nm thick) are grown at 285 K, which corresponds to 0.85 T_g for TPD and 0.67 T_g for TCTA. Therefore, TPD is grown as a highly stable glass, whereas the stability of TCTA is still much higher than the one of the ordinary glass (cooled at -10 K/min) [8,9]. The growth rate is fixed at 0.08 nm/s for both materials. Once the three-layer stack (TCTA-TPD-TCTA) is grown onto the Al plate of our calorimetric chip we isothermally anneal it for various times at annealing temperatures ranging from $T_g + 14$ to $T_g + 34$ K. After annealing, the sample is passively cooled at around -500 K/s down to $T = 200$ K. Next, the calorimeter is immediately scanned at a heating rate around 3.5×10^4 K/s to temperatures well above the onset of devitrification of the stable glass [see schematics of Fig. 1(a)]. For comparison, we also analyze the bulk transformation of 35 μm thick TPD films, grown under identical conditions as the thinner layers, but without using capping layers of TCTA. Calorimetric measurements for the thick samples are conducted on glasses annealed at $T_g + 14$ K using heating and cooling rates of 10 K/min in a Perkin-Elmer DSC 7. In this case, the quantity transformed by a moving front from the surface is previously subtracted to estimate the transformation due to the bulk mechanism.

Figure 1 shows the specific heat capacity c_{sp} curves measured after annealing a capped TDP thin film at $T_g +$ 29 K for times up to 70 s. The black continuous curve in Fig. 1(a) represents the specific heat obtained on heating the as-deposited stack. The large overshoot with peak temperature $T_{\mathrm{peak}}(\mathrm{SG}) = 428$ K is the bulk devitrification of the stable TPD glass. The red curve corresponds to a sample fully transformed after an isotherm at $T_g + 29$ K for 65 s and the endothermic peak at low temperature ($T_{\mathrm{peak(FC)}} \approx 372$ K) originates from the complete devitrification of the glass that is subsequently fast cooled from the liquid state (FC glass). The broad feature at higher temperatures is the remaining TCTA that has not yet transformed during the previous isotherm. The heat capacity of the samples annealed at intermediate times ($0 < t < t_{\mathrm{max}}$) shows several devitrification peaks. Two main features can be highlighted: (i) the area increase over time of the endothermic peak of the FC glass and (ii) a continuous decrease of the intensity and a shift towards lower temperatures of the high temperature endotherm. These features

reveal that the bulk transformation of the stable glass proceeds through two parallel competing processes: transformation of part of the glass into a SCL that upon cooling forms a FC glass and partial rejuvenation or softening of the stable glass, that is, the remaining stable glass loses stability continuously as time increases when annealed above its limiting fictive temperature. Similar specific heat data for other annealing temperatures are shown in the Supplemental Material [22] Figs. SM1 and SM2 for capped thin films and for the thick sample, respectively. The transformed fraction x_l and the relative variation of $T_{\mathrm{peak}}(\mathrm{SG})$, expressed as $\Delta T_{\mathrm{peak}}(t)/\Delta T_{\mathrm{max}}$, where $\Delta T_{\mathrm{peak}}(t) = T_{\mathrm{peak}}(\mathrm{AD}) - T_{\mathrm{peak}}(t)$ and $\Delta T_{\mathrm{max}} = T_{\mathrm{peak}}(\mathrm{AD}) - T_{\mathrm{peak}}(\mathrm{FC})$ for the sample annealed at $T_g + 29$ K, are plotted in Fig. 1(b). The protocol used to estimate the transformed fraction from the c_{sp} curves can be found in the Supplemental Material [22]. The data have a sigmoidal shape as typically observed for the kinetics of first-order phase transitions such as crystallization or melting [23]. The small variation of T_{peak} after 33 s of annealing $[\Delta T_{\mathrm{peak}}(t)/\Delta T\ \mathrm{max}] = 0.2$ with $\Delta T_{\mathrm{peak}}(t) = 11$ K and $\Delta T_{\mathrm{max}} = 54.5$ K with respect to the increase of x_l at the same time (65%–70% at $t = 33$ s), indicates softening is a slower process than the transformation into the SCL. In other words, the untransformed stable glass is still a very stable glass up to its complete transformation into the liquid by the nucleation-and-growth mechanism.

The transformed fractions as a function of time for the four isotherms are displayed in Fig. 2(a). We interpret our data using the KJMAE equation $x_l = 1 - \exp(x_{\mathrm{ext}}) = 1 - \exp[-(Kt)^n]$. x_l is the real liquid fraction while x_{ext} denotes the extended fraction which does not consider impingement between nuclei of the new phase. The derivation of this equation and the expression of x_{ext} according to the mechanism of the transformation and the dimensionality are presented in the Supplemental Material [22]. In this model the mechanism and the main parameters of the transformation are encoded in K and in the exponent n (see Supplemental Material [22] for details). The data of Fig. 2(a) can be represented in a $\ln[-\ln(1 - x_l)]$ vs $\ln(t)$ plot that highlights graphically the value of the average exponent n for both the thin and thick layers. This is shown in Fig. 2(b) where the plot is normalized by the time required to transform the sample (t_{max}) and the data for the thin films collapse into a master curve. The experimental value of $n = 2.02 \pm 0.04$ for the thin capped TPD layers is consistent with a 2D growth with zero nucleation frequency, that is the initiation sites of the transformation already exist at $t = 0$. If the nucleation frequency was constant over time the exponent for a 2D growth would be three instead of two (see Supplemental Material [22]). The bulk sample (35 μm thick) transforms with $n = 3.0 \pm 0.2$ in agreement with a 3D growth with zero nucleation frequency (see Supplemental Material [22]). The origin of the difference in the exponent n between thin and thick layers is discussed below.

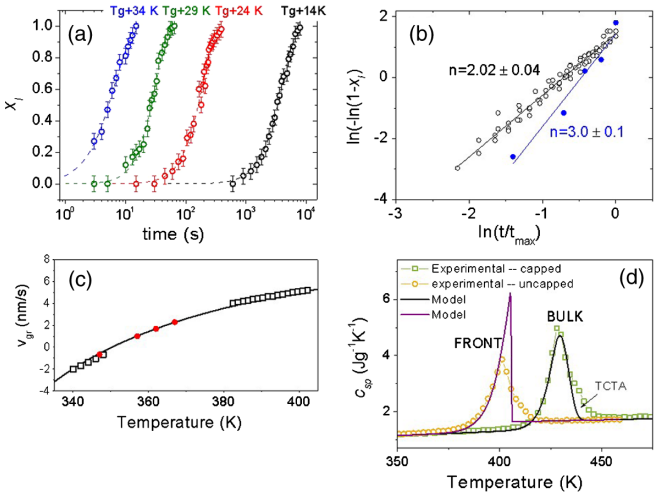

FIG. 2. (a) Transformed fraction vs the logarithm of the transformation time at four different temperatures. Dashed line, fittings obtained by the KJMAE equation. (b) $\ln[-\ln(1 - \boldsymbol{x_l})]$ vs logarithm of the transformation time normalized by t_{max} for both thick and capped thin films. (c) Growth front velocity vs temperature for TPD stable glasses. TPD data from Ref. [24]. The red symbols represent data used for the KJMAE fitting. (d) Specific heat measured by nanocalorimetry at 3.5×10^4 K/s of a thin film (orange open circles) that transforms by front and a capped layer (open green squares) that transforms by bulk together with the calculated c_{sp} (continuous lines) using values derived from isothermal measurements.

The data of Fig. 2(a) are also fitted individually with the KJMAE equation (dashed lines). The best fitting parameters, the number of preexisting sites N, and the exponent n are shown in Table I. The propagation velocity of the moving fronts at each temperature [red circles in Fig. 2(c)] is taken from data of the growth front velocity v_{gr}, previously measured for the front transformation of stable TPD glasses [21, 24]. It is known that vapor-deposited glasses develop distinct anisotropic molecular orientations depending on the deposition temperature [25]. However, given that the tendency to molecular orientation along the substrate plane is relatively small for TPD glasses grown at 0.85 Tg, we assume the growth front velocity of the liquid patches is nearly isotropic in this glass [26].

The exponent n ranges from 1.8 to 2.2 for the capped layers and amounts to 3.4 for the bulk sample, while the average spatial distance between initiation sites in the thin glassy layers $\langle d \rangle$ varies from 1.6 to 3.4 μm, average value of 2.5 ± 1 μm, without a clear trend with the annealing temperature. The value for the thick film 2.5 μm lies in the same range. $\langle d \rangle$ is evaluated through the expression $N^{-(1/D)}$, being D the dimension.

The giant length scale associated with the distance between the initiation sites is one of the main and more surprising results in terms of glass physics. It, however,

TABLE I. Values of the parameters used in the KJMAE equation to generate dashed lines in Fig. 2(a) and Fig. SM2 for the thick TPD glass. $D = 2$ in 2D and $D = 3$ in 3D.

	T_{anneal}	v_{gr} (nm/s)	n	K (s^{-1})	N (nuclei/m^D)	$\langle d \rangle$ (μm)
Thin films 85 nm (2D)	$Tg + 14$ K	0.22	2.0 ± 0.25	$(2.48 \pm 0.16)E\text{-}4$	$(4.06 \pm 0.52)E11$	1.57 ± 0.10
	$Tg + 24$ K	10.0	2.08 ± 0.30	$(5.23 \pm 0.70)E\text{-}3$	$(8.7 \pm 2.3)E10$	3.40 ± 0.46
	$Tg + 29$ K	48.2	2.23 ± 0.34	$(3.19 \pm 0.25)E\text{-}2$	$(1.39 \pm 0.22)E11$	2.68 ± 0.21
	$Tg + 34$ K	193.8	1.80 ± 0.34	0.15 ± 0.01	$(1.92 \pm 0.25)E11$	2.28 ± 0.15
Bulk 35 μm (3D)	$Tg + 14$ K	0.22	3.37 ± 0.23	$(1.40 \pm 0.04)E\text{-}4$	$(6.16 \pm 0.13)E16$	2.53 ± 0.07

roughly agrees with the estimation of earlier work [7], with recent simulations on stable computer-generated glasses [12,13] and compares well with the crossover length for the front-to-bulk transition in highly stable TPD glasses measured in independent experiments [24]. The transition from 2D to 3D growth between 85 nm and 35 μm thick films is a consequence of the average distance between initiation sites $\langle d \rangle \approx 2.5$ μm. When the thickness of the TPD layer (85 nm) is much lower than $\langle d \rangle$, the nuclei reach the final vertical dimension shortly after its formation and its growth proceeds laterally in 2D over time. On the contrary, the bulk sample has a thickness much larger than $\langle d \rangle$ and the liquid patches grow simultaneously in all directions (3D growth). $\langle d \rangle/2$ is also in agreement within experimental uncertainty with the crossover length parameter evaluated from a model that considers the recovery to equilibrium is driven by the mismatch in the dynamics between glass and liquid and also agrees with experimental data independently measured by standard calorimetry.

The validity of the approach is tested calculating the specific heat under continuous heating from the data obtained during the isotherms. The Cp calculation is detailed in the Supplemental Material [22] and the results are shown in Fig. 2(d). Data points correspond to experimental data, while solid lines are calculations based on the parameters listed in Table I but using the KJMAE model applied to temperature scans. The agreement of the onset of the transformation of the calculated Cp curves with the experimental calorimetric traces measured with fast-scanning nanocalorimetry is remarkable for both the surface and bulklike processes. This confirms that both mechanisms can be understood using similar growth front velocities that mainly depend on temperature $v_{\text{gr}}(\text{T})$. We note that the simultaneous partial rejuvenation of the highly stable glass does not seem to play a significant role in the transformation process of the highly stable glass at these high heating rates.

The difference between the surface and bulk processes is indeed related to the initiation sites of the transformation. As already suggested by Gutierrez *et al.* [10] the separation distance between the nucleation sites controls the transformation. In thin films of a thickness below the crossover length and with free surfaces and interfaces the front propagates from the surface at $v_{\text{gr}}(\text{T})$. In much thicker stable glasses there is also a moving front starting at the surface but at the same time the front propagates at the same $v_{\text{gr}}(\text{T})$ radially outwards from the many preexisting seeds located in the interior of the material. This second process is dominant due to the large quantity of initiation sites.

Unfortunately, calorimetry does not provide any direct microscopic evidence of the nature of the initiation sites. Further experiments by small angle x-ray scattering or related techniques may be useful to identify them. At this stage, we can only speculate about its origin: (i) regions with lower density that are randomly distributed but spatially separated by few microns, or (ii) regions that become active at the annealing temperature and transform into liquid. In this view the material has a broad distribution of local fictive temperatures and once a local region becomes highly mobile dynamic facilitation eases its propagation to neighboring regions with higher local T_f. This view is supported by RFOT or dynamic facilitation theories. However, we emphasize that within experimental uncertainty we do not observe a strong dependence of the number of "transformation sites" with the annealing temperature.

In summary, the bulk transformation of ultrastable glasses into the supercooled liquid proceeds through a nucleation and growth process that becomes dominant for films much thicker than the crossover length. The partial rejuvenation of the ultrastable glass, although present, does not have a significant impact on the growth front velocity and therefore does not affect the transformation process. The exponents associated with the transformed fraction, $n \approx 2$ and $n \approx 3$ for thin and thick films, respectively, correlate with the 2D or 3D nature of the transformation and indicate the nucleation is highly heterogeneous starting at preexisting seeds already present at $t = 0$. Surprisingly, the density of these initiation sites appears to be independent of the melting temperature. The transformation then proceeds by moving fronts that propagate with a velocity that matches the one measured for the front transformation. The large distance between them, on the micron length scale, determines the crossover length of the transformation.

This work has been partially supported by the Spanish Ministry of Economy and Competitiveness, MINECO, through Project No. MAT2016-79579-R. J. R.-R. also thanks the Spanish Ministry of Education, Culture and Sport for its financial support within the FPU program.

The authors declare no competing financial interests.

*Present address: The Organic Photonics and Electronics Group, Department of Physics, Umeå University, SE-90187 Umeå, Sweden.
†Corresponding author.
javier.rodriguez@uab.cat

[1] V. Lubchenko and P. G. Wolynes, Annu. Rev. Phys. Chem. **58**, 235 (2007).
[2] C. T. Moynihan, A. J. Easteal, M. A. Bolt, and J. Tucker, J. Am. Ceram. Soc. **59**, 12 (1976).
[3] F. Ritort and P. Sollich, Adv. Phys. **52**, 219 (2003).
[4] T. R. Kirkpatrick, D. Thirumalai, and P. G. Wolynes, Phys. Rev. A **40**, 1045 (1989).
[5] A. S. Keys, J. P. Garrahan, and D. Chandler, Proc. Natl. Acad. Sci. U.S.A. **110**, 4482 (2013).
[6] A. Wisitsorasak and P. G. Wolynes, J. Phys. Chem. B **118**, 7835 (2014).
[7] K. L. Kearns, M. D. Ediger, H. Huth, and C. Schick, J. Phys. Chem. Lett. **1**, 388 (2010).
[8] C. Rodríguez-Tinoco, M. Gonzalez-Silveira, J. Ràfols-Ribé, A. F. Lopeandía, M. T. Clavaguera-Mora, and J. Rodríguez-Viejo, J. Phys. Chem. B **118**, 10795 (2014).
[9] J. Ràfols-Ribé, A. Vila-Costa, C. Rodríguez-Tinoco, A. F. Lopeandia, J. Rodríguez-Viejo, and M. Gonzalez-Silveira, Phys. Chem. Chem. Phys. **20**, 29989 (2018).
[10] R. Gutiérrez and J. P. Garrahan, J. Stat. Mech. (2016) 074005.
[11] P. G. Wolynes, Proc. Natl. Acad. Sci. U.S.A. **106**, 1353 (2009).
[12] R. L. Jack and L. Berthier, J. Chem. Phys. **144**, 244506 (2016).
[13] E. Flenner, L. Berthier, P. Charbonneau, and C. J. Fullerton, Phys. Rev. Lett. **123**, 175501 (2019).
[14] A. Ninarello, L. Berthier, and D. Coslovich, Phys. Rev. X **7**, 021039 (2017).
[15] S. F. Swallen, K. L. Kearns, M. K. Mapes, Y. S. Kim, R. J. McMahon, M. D. Ediger, T. Wu, L. Yu, and S. Satija, Science **315**, 353 (2007).
[16] E. Leon-Gutierrez, A. Sepúlveda, G. Garcia, M. T. Clavaguera-Mora, and J. Rodríguez-Viejo, Phys. Chem. Chem. Phys. **12**, 14693 (2010).
[17] A. N. Kolmogorov, Bull. Acad. Sci. USSR, Phys. Ser. **1**, 355 (1937).
[18] W. A. Johnson and R. F. Mehl, Trans. Am. Inst. Min. Metall. Eng. **135**, 416 (1939).
[19] M. Avrami, J. Chem. Phys. **7**, 1103 (1939).
[20] M. Avrami, J. Chem. Phys. **8**, 212 (1940).
[21] A. Sepúlveda, S. F. Swallen, and M. D. Ediger, J. Chem. Phys. **138**, 12A517 (2013).
[22] See Supplemental Material at http://link.aps.org/supplemental/10.1103/PhysRevLett.124.076002 for complementary experimental data and an explanation of the calculation of the transformed fraction and the simulated heat capacity curves. A Monte Carlo model reproducing the nucleation and growth process is also discussed.
[23] M. T. Clavaguera-Mora, N. Clavaguera, D. Crespo, and T. Pradell, Prog. Mater. Sci. **47**, 559 (2002).
[24] C. Rodríguez-Tinoco, M. Gonzalez-Silveira, J. Ràfols-Ribé, A. Vila-Costa, J. C. Martinez-Garcia, and J. Rodríguez-Viejo, Phys. Rev. Lett. **123**, 155501 (2019).
[25] S. S. Dalal, D. M. Walters, I. Lyubimov, J. J. de Pablo, and M. D. Ediger, Proc. Natl. Acad. Sci. U.S.A. **112**, 4227 (2015).
[26] C. Rodríguez-Tinoco, M. Gonzalez-Silveira, J. Ràfols-Ribé, A. F. Lopeandía, and J. Rodríguez-Viejo, Phys. Chem. Chem. Phys. **17**, 31195 (2015).